



Geo-neutrino energy spectrum and its implication



Yu-Feng Li (李玉峰)

Institute of High Energy Physics, Beijing

liyufeng@ihep.ac.cn

Introduction



1. Geoneutrino spectrum is the basis for geoneutrino sensitivity study

2. Old flux model: Enomoto's model

• ENSDF 2005



ENSDF 2023

• Single beta branch

- Only allowed transition
- Without high-order corrections



Should be included

Geoneutrino flux

IBD cross section



Predicted signals (rate and shape)

3. Spectral impact to analysis

Observed data: KamLAND (2022), Borexino (2020)

Predicted data: JUNO

Geoneutrinos: Introduction

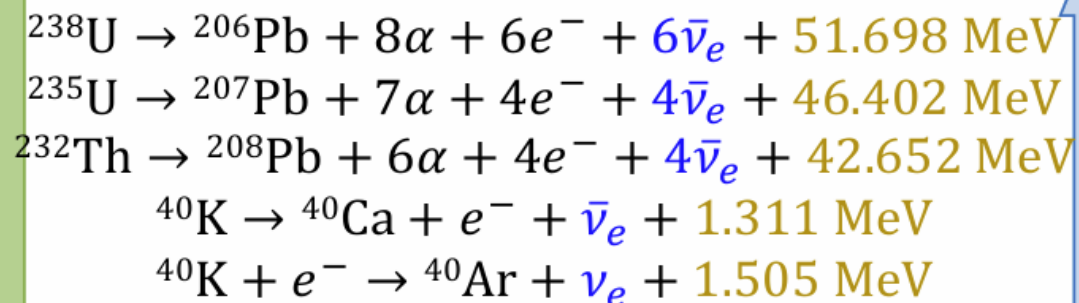


Geoneutrino

- The intersection of **particle physics** and **geophysics**
- An independent method to study the matter composition deep within the Earth

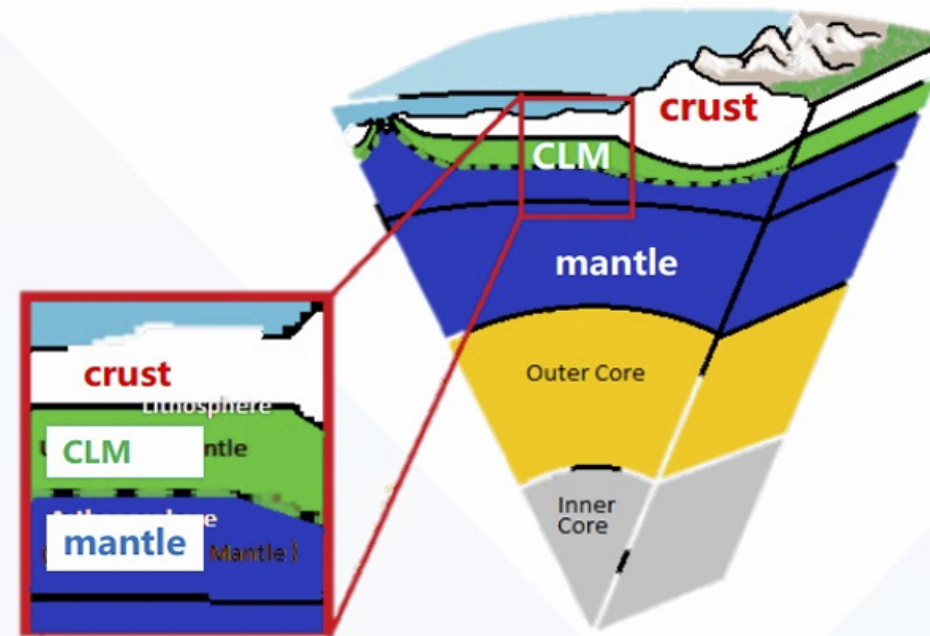
Abundance of the radioactive elements

Radiogenic heat



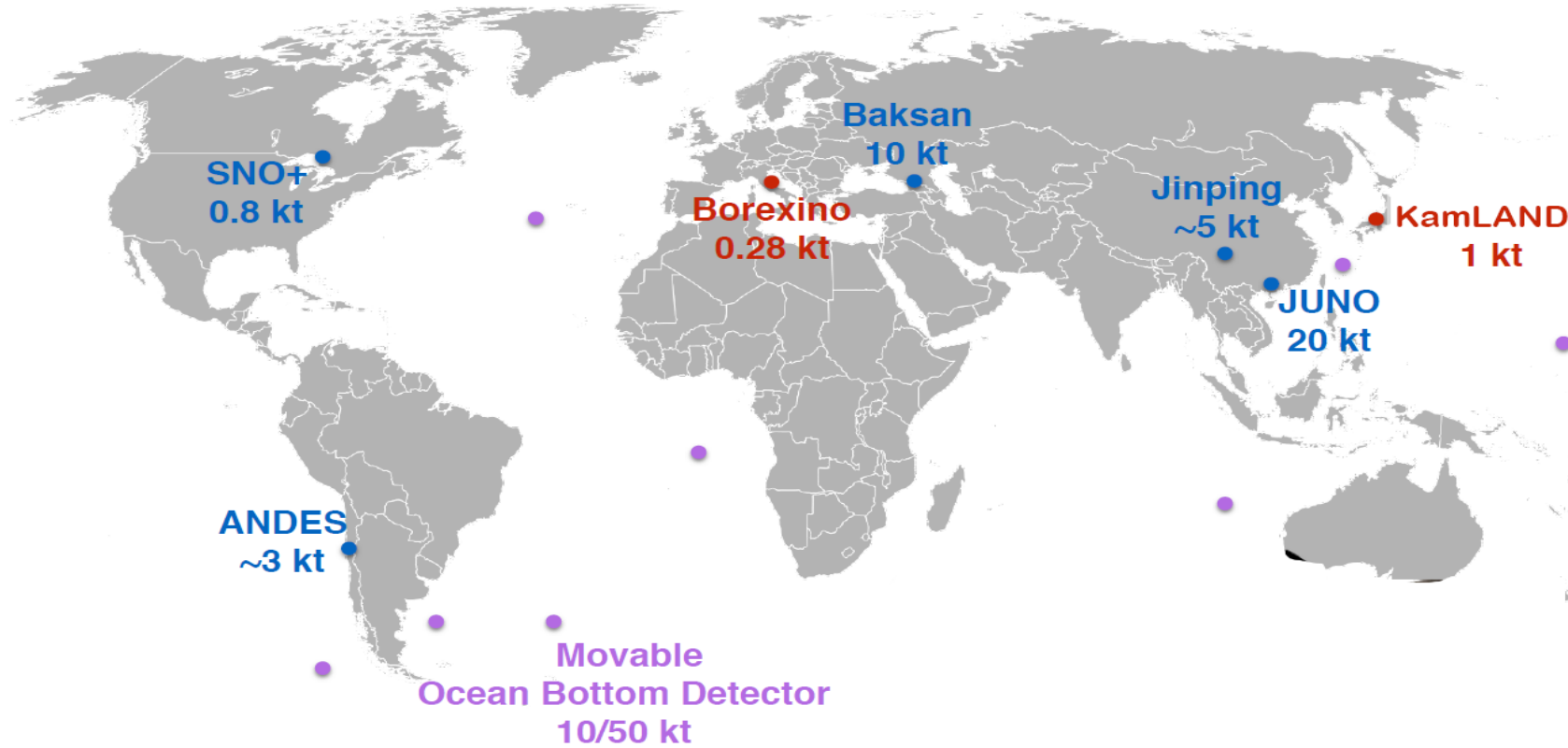
Geo-neutrino flux

$$S_{\text{Total}} = S_{\text{Crust}} + S_{\text{CLM}} + S_{\text{Mantle}}$$



- **Crust**: high U & Th
- **CLM (Continental Lithospheric Mantle)**: relatively low U & Th
- **Mantle**: very low U & Th, large volume

Geoneutrino Observation

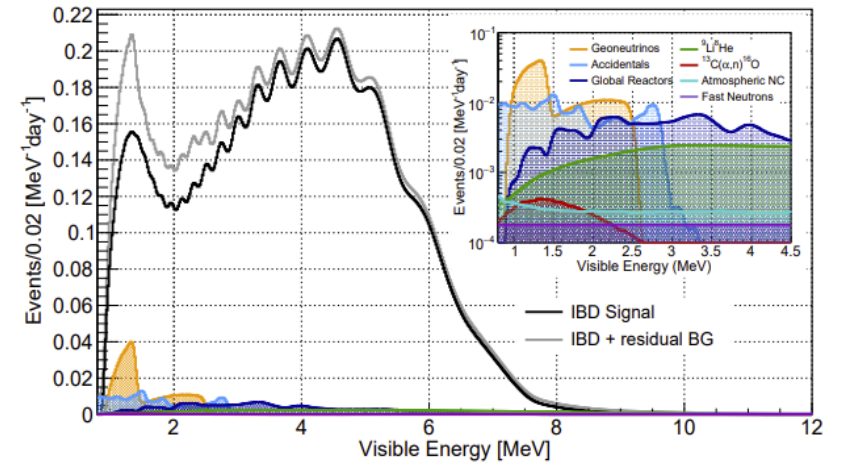
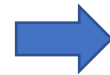
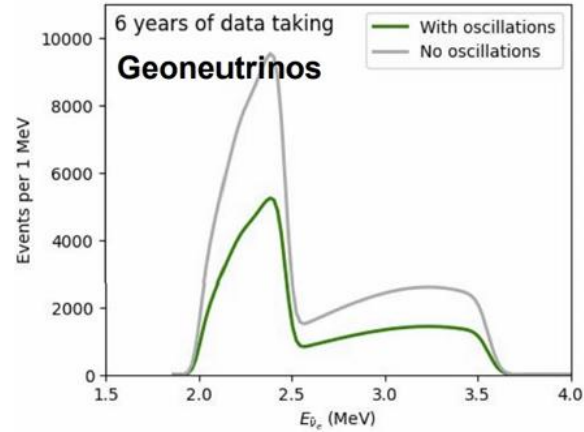
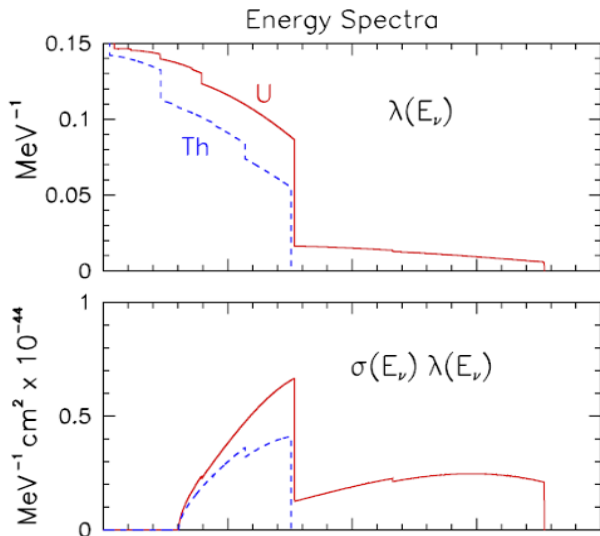


Motivation for precise spectral calculation



➤ Liquid scintillator detectors lack of directionality

→ The energy spectral feature of **both geoneutrinos and reactor neutrinos** is important !



*JUNO collaboration,
2204.13249*

The new geoneutrino flux model

(Li & Xin, arXiv: 2412.07711):

Summation model with latest database,
higher order corrections and forbidden decays

Geo-neutrino flux: the new calculation



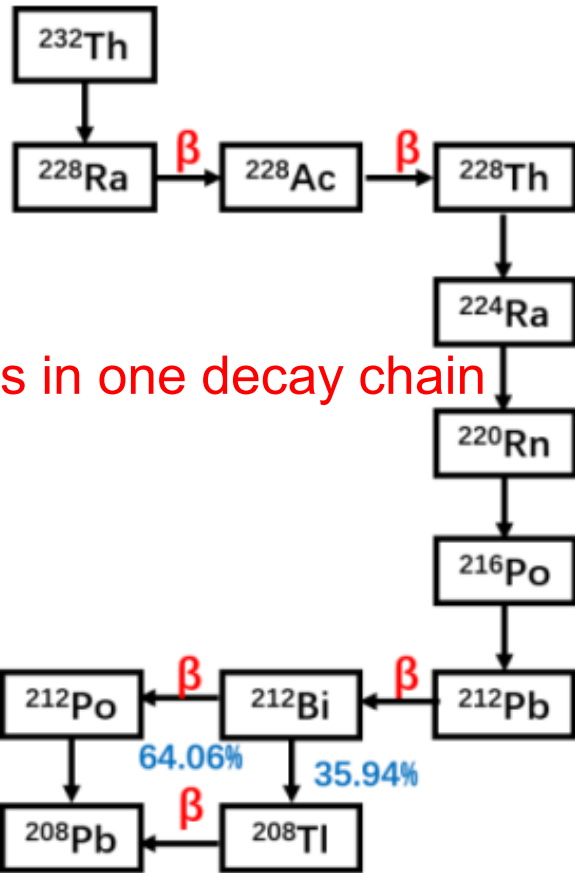
A single decay branch

Fermi's golden rule
(modern calculation)

$$S_{\bar{\nu}}^k(E_{\bar{\nu}}) = \underbrace{K}_{\text{Normalization}} p_{\bar{\nu}} E_{\bar{\nu}} (E_0^k - E_{\bar{\nu}})^2 \underbrace{F(Z, E_{\bar{\nu}})}_{\text{Fermi function}} \underbrace{C(E_{\bar{\nu}})}_{\text{Shape factor}} [1 + \underbrace{\delta_{\bar{\nu}}(Z, A, E_{\bar{\nu}})}_{\text{Corrections}}]$$

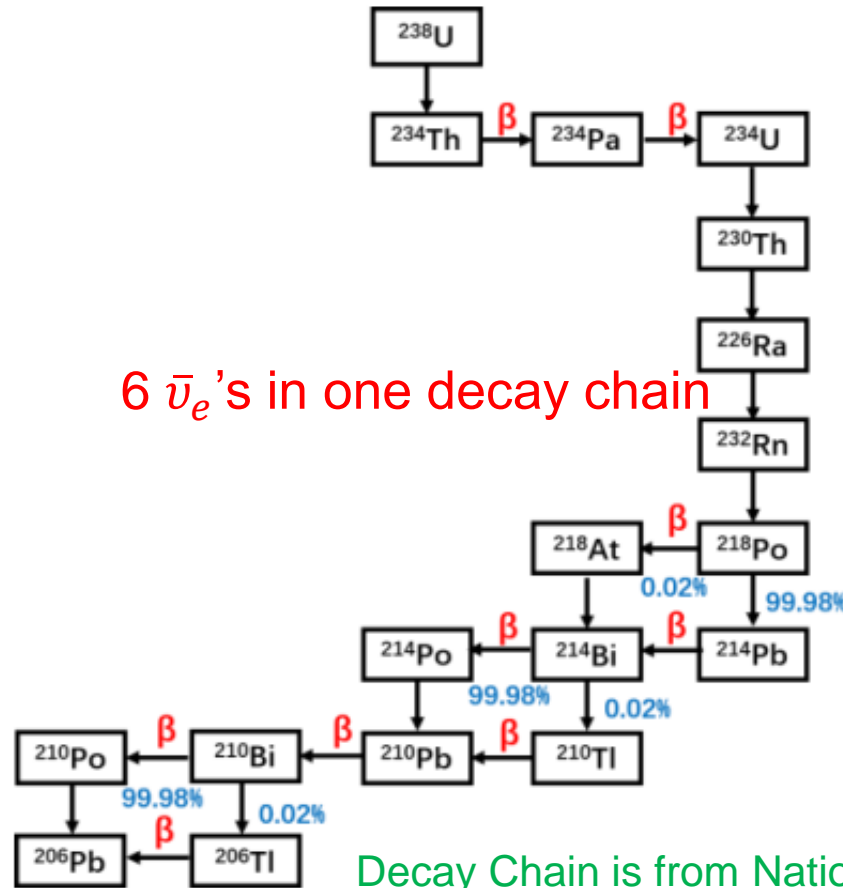
radiative corrections
weak magnetism
finite size

Decay chain for ^{232}Th



4 $\bar{\nu}_e$'s in one decay chain

Decay chain for ^{238}U



6 $\bar{\nu}_e$'s in one decay chain

Single branch calculation follows
[Phys.Rev.D 100 \(2019\) 5, 053005](#)
[YFL, Zhang](#)

nuclide i → nuclide j
whole decay chain

$$S_X(E_{\bar{\nu}}) = \sum_{ij} R_{ij} \sum_k I_k S_{\bar{\nu}}^k(E_{\bar{\nu}})$$

branch ratio

Decay information is taken
from ENSDF database

Decay Chain is from National Nuclear Data Center

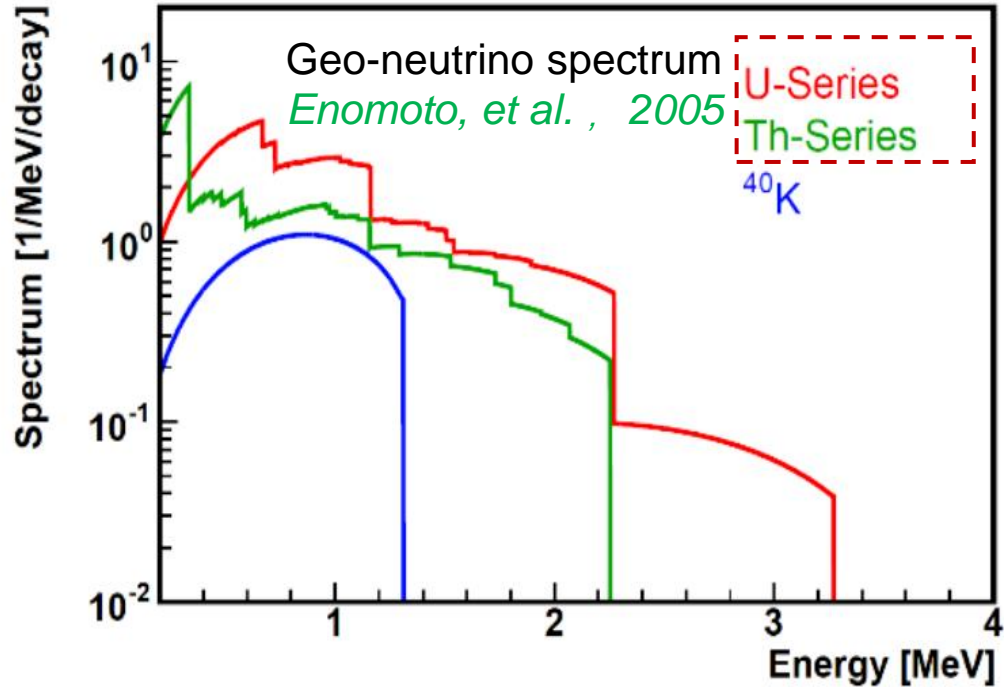
Geo-neutrino flux: Enomoto's flux



Enomoto's flux model

$$S_{\bar{\nu}}^k(E_{\bar{\nu}}) = \underbrace{K}_{\text{Normalization}} p_{\bar{\nu}} E_{\bar{\nu}} (E_0^k - E_{\bar{\nu}})^2 \underbrace{F(Z, E_{\bar{\nu}})}_{\text{Fermi function}} \underbrace{C(E_{\bar{\nu}})}_{\text{Shape factor}} [1 + \underbrace{\delta_{\bar{\nu}}(Z, A, E_{\bar{\nu}})}_{\text{Corrections}}]$$

- ~~radiative corrections~~
- ~~weak magnetism~~
- ~~finite size~~



currently used in most of studies

<https://www.awa.tohoku.ac.jp/~sanshiro/research/geoneutrino/spectrum/>

Differences between the Enomoto's and new fluxes

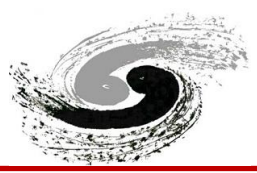
	Enomoto flux	New flux
Database	ENSDF 2005	ENSDF 2023
Single branch	Only allowed transition	<ul style="list-style-type: none"> forbidden decays High order corrections

Database:

	ENSDF 2005	ENSDF 2023
²³⁸ U → ²⁰⁸ Pb	82 (12)	159 (12) <small>total transitions (effective transitions)</small>
²³² Th → ²⁰⁶ Pb	70 (3)	84 (3)

The extra beta branches are concentrated in the **low-energy region**, less than the **IBD threshold**.

Geo-neutrino flux: visible transitions



$i \rightarrow j$	R_{ij}	Q -value [keV]	transition number
$^{234}\text{Th} \rightarrow ^{234}\text{Pa}$	1.0000	199.5	5 (0)
$^{234}\text{Pa}^m \rightarrow ^{234}\text{U}$	0.9984	2290.0	24 (1)
$^{214}\text{Pb} \rightarrow ^{214}\text{Bi}$	0.9998	1018.0	7 (0)
$^{214}\text{Bi} \rightarrow ^{214}\text{Po}$	0.9998	3269.0	70 (6)
$^{210}\text{Pb} \rightarrow ^{210}\text{Bi}$	1.0000	63.5	2 (0)
$^{210}\text{Bi} \rightarrow ^{210}\text{Po}$	0.9999	1161.5	1 (0)
$^{234}\text{Pa} \rightarrow ^{234}\text{U}$	0.0016	1247	39 (0)
$^{218}\text{Po} \rightarrow ^{218}\text{At}$	0.0002	264.0	1 (0)
$^{206}\text{Tl} \rightarrow ^{206}\text{Pb}$	0.0001	1532.3	3 (0)
$^{210}\text{Tl} \rightarrow ^{210}\text{Pb}$	0.0002	4386.0	7 (5)

TABLE IV: Beta decay transitions in the ^{238}U chain. For each transition, the weight of the production ratio R_{ij} , the Q -value, and the number of decay branches are provided. The last column lists the total number of decay branches as well as the effective decay branches that can be detected by the IBD reaction.

$i \rightarrow j$	R_{ij}	Q -value [keV]	transition number
$^{228}\text{Ra} \rightarrow ^{228}\text{Ac}$	1.0000	39.5	4 (0)
$^{228}\text{Ac} \rightarrow ^{228}\text{Th}$	1.0000	2076.0	55 (2)
$^{212}\text{Pb} \rightarrow ^{212}\text{Bi}$	1.0000	569.1	3 (0)
$^{212}\text{Bi} \rightarrow ^{212}\text{Po}$	0.6406	2251.5	7 (1)
$^{208}\text{Tl} \rightarrow ^{208}\text{Pb}$	0.3594	1801.3	15 (0)

TABLE V: Beta decay transitions in the ^{232}Th chain. For each transition, the weight of the production ratio R_{ij} , the Q -value, and the number of decay branches are provided. The last column lists the total number of decay branches as well as the effective decay branches that can be detected by the IBD reaction.

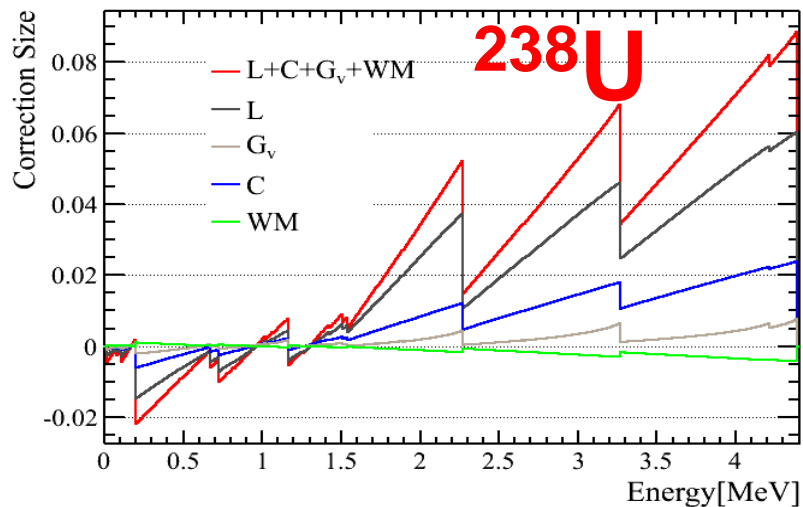
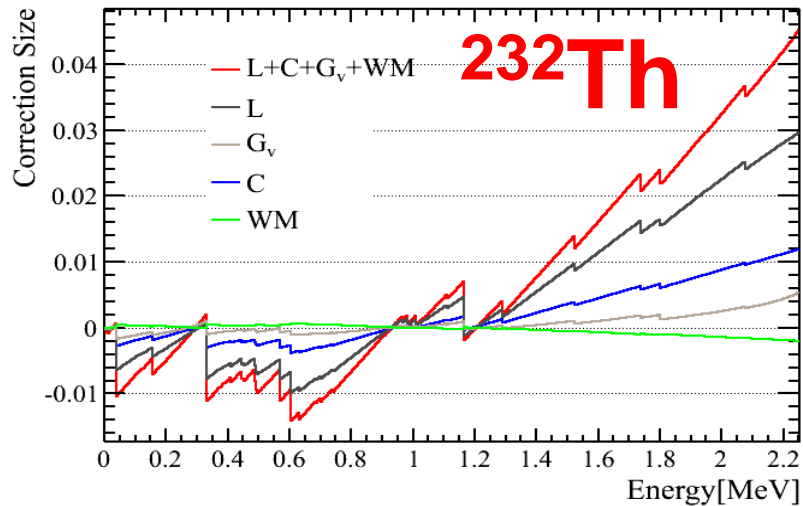
Geo-neutrino flux: visible branches



decay chains	$i \rightarrow j$	$R_{i,j}$	Q -value [keV]	$I_{i,j,k}$	$\delta I_{i,j,k}$	Transition type
^{238}U	$^{234}\text{Pa}^m \rightarrow ^{234}\text{U}$	1.0000	2290.0	0.9757	0.0004	1 st forbidden ($0^- \rightarrow 0^+$)
			3269.0	0.192	0.004	1 st forbidden ($1^- \rightarrow 0^+$)
	$^{214}\text{Bi} \rightarrow ^{214}\text{Po}$	0.9998	2660.0	0.0055	0.0008	1 st forbidden ($1^- \rightarrow 2^+$)
			2254.0	0.00079	0.00013	3 rd forbidden ($1^- \rightarrow 4^+$)
			1994.0	0.0006	0.0004	2 nd forbidden ($1^- \rightarrow 3^-$)
			1891.0	0.0722	0.0008	1 st forbidden ($1^- \rightarrow 2^+$)
			1854.0	0.009	0.0005	1 st forbidden ($1^- \rightarrow 0^+$)
	$^{210}\text{Tl} \rightarrow ^{210}\text{Pb}$	0.0002	4386.0	0.20	Unknown	Allowed ($5^+ \rightarrow 4^+$)
			4210.0	0.30	0.06	2 rd forbidden ($5^+ \rightarrow 8^+$)
			2413.0	0.10	0.03	2 rd forbidden ($5^+ \rightarrow 2^+$)
2020.0			0.10	0.03	Allowed ($5^+ \rightarrow 4^+$)	
1860.0			0.24	0.05	Unknown	
^{232}Th	$^{212}\text{Bi} \rightarrow ^{212}\text{Po}$	0.6406	2251.5	0.8643	0.0012	1 st forbidden ($1^- \rightarrow 0^+$)
			2076.0	0.07	0.05	Allowed ($3^+ \rightarrow 2^+$)
	$^{228}\text{Ac} \rightarrow ^{228}\text{Th}$	1.0000	1947.0	0.006	0.005	Allowed ($3^+ \rightarrow 4^+$)

TABLE VI: Effective transitions above the IBD threshold in the decay chains of ^{238}U and ^{232}Th . In addition to the R_{ij} and Q -values provided in Table IV and V, the intensity $I_{i,j,k}$, its uncertainty $\delta I_{i,j,k}$, and the transition type are also listed. These values are obtained from the latest ENSDF nuclear database [23].

Geo-neutrino flux update: decomposition



➤ Corrections from:
Finite size, radiative correction, and weak magnetism

➤ Corrections from:
Forbidden decays (shape factor)

Classification	ΔJ^π	Operator	Shape Factor $C(E_e)$		WM correction $\delta_{WM}(E_e)$
			Plane wave approximation	Exact relativistic calculation	
Allowed GT	1^+	$\Sigma \equiv \sigma\tau$	1	1	$\frac{2}{3} \frac{\mu_\nu - 1/2}{M_{NSA}} (E_e \beta^2 - E_\nu)$
Nonunique first forbidden GT	0^-	$[\Sigma, r]^{0-}$	$p_e^2 + E_\nu^2 + 2\beta^2 E_\nu E_e$	$E_\nu^2 + p_e^2 \tilde{F}_{p_{1/2}} + 2p_e E_\nu \tilde{F}_{sp_{1/2}}$	0
Nonunique first forbidden GT	1^-	$[\Sigma, r]^{1-}$	$p_e^2 + E_\nu^2 - \frac{4}{3}\beta^2 E_\nu E_e$	$E_\nu^2 + \frac{2}{3}p_e^2 \tilde{F}_{p_{1/2}} + \frac{1}{3}p_e^2 \tilde{F}_{p_{3/2}} - \frac{4}{3}p_e E_\nu \tilde{F}_{sp_{1/2}}$	$\frac{\mu_\nu - 1/2 (E_e \beta^2 - E_\nu)(p_e^2 + E_\nu^2) + 2\beta^2 E_e E_\nu (E_\nu - E_e)/3}{M_{NSA} (p_e^2 + E_\nu^2 - 4\beta^2 E_\nu E_e/3)}$
Unique first forbidden GT	2^-	$[\Sigma, r]^{2-}$	$p_e^2 + E_\nu^2$	$E_\nu^2 + p_e^2 \tilde{F}_{p_{3/2}}$	$\frac{3}{5} \frac{\mu_\nu - 1/2 (E_e \beta^2 - E_\nu)(p_e^2 + E_\nu^2) + 2\beta^2 E_e E_\nu (E_\nu - E_e)/3}{M_{NSA} (p_e^2 + E_\nu^2)}$

$$\tilde{F}_{p_{3/2}}(E_e, R) \simeq F_1(E, Z)/F_0(E, Z),$$

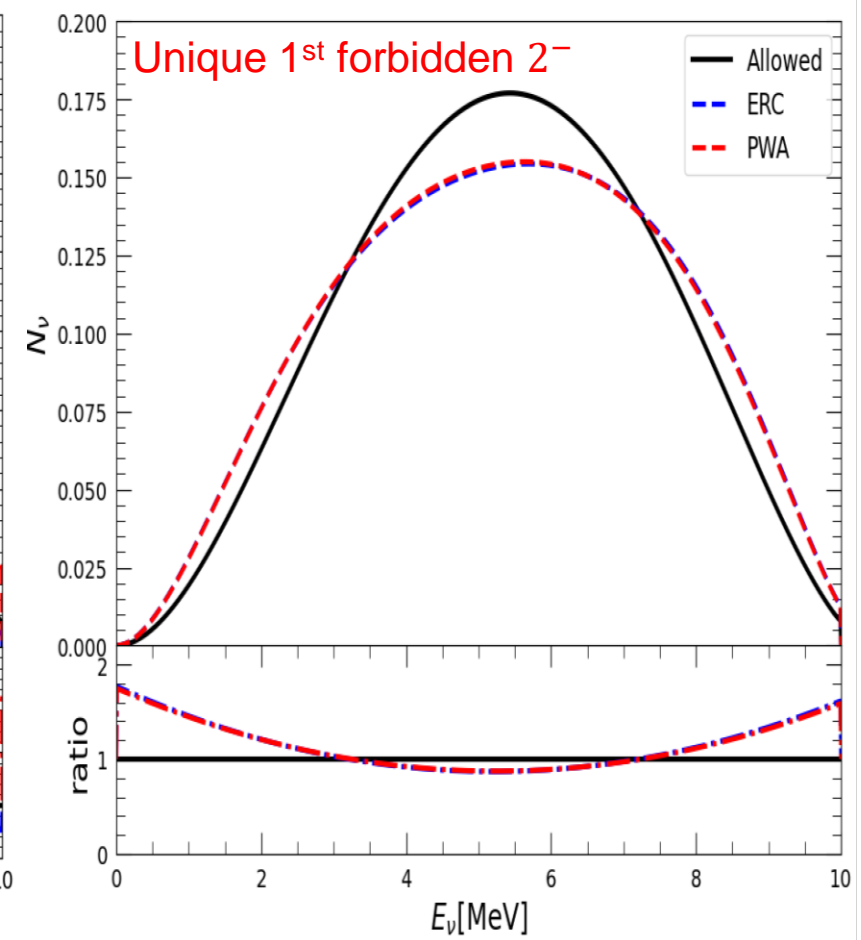
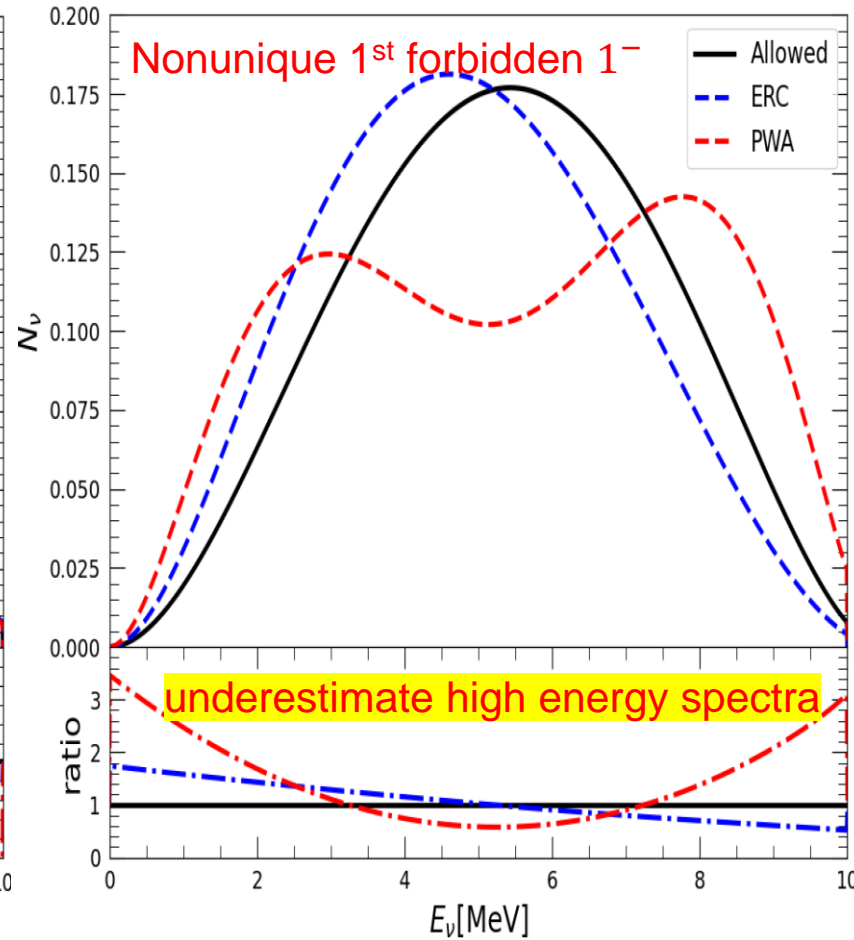
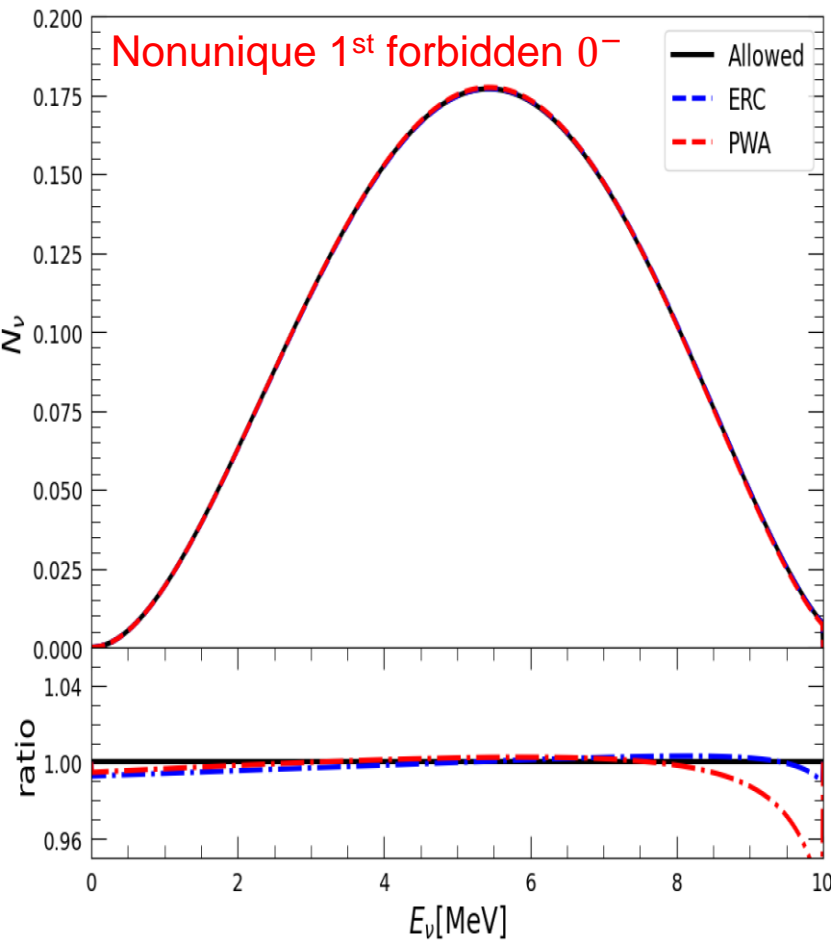
$$\tilde{F}_{p_{1/2}}(E_e, R) \simeq \left[\left(\frac{\alpha Z}{2} + \frac{E_e R}{3} \right)^2 + \left(\frac{m_e R}{3} \right)^2 - \frac{2m_e^2 R}{3E_e} \left(\frac{\alpha Z}{2} + \frac{E_e R}{3} \right) \right] / j_1^2(p_e R)$$

$$\tilde{F}_{sp_{1/2}}(E_e, R) \simeq \left[\left(\frac{\alpha Z}{2} + \frac{E_e R}{3} \right) - \frac{m_e^2 R}{3E_e} \right] / (j_0(p_e R) j_1(p_e R)),$$

Stefanik, Dvornicky and Simkovic (2017)

Using corrections of Huber P, (2011)

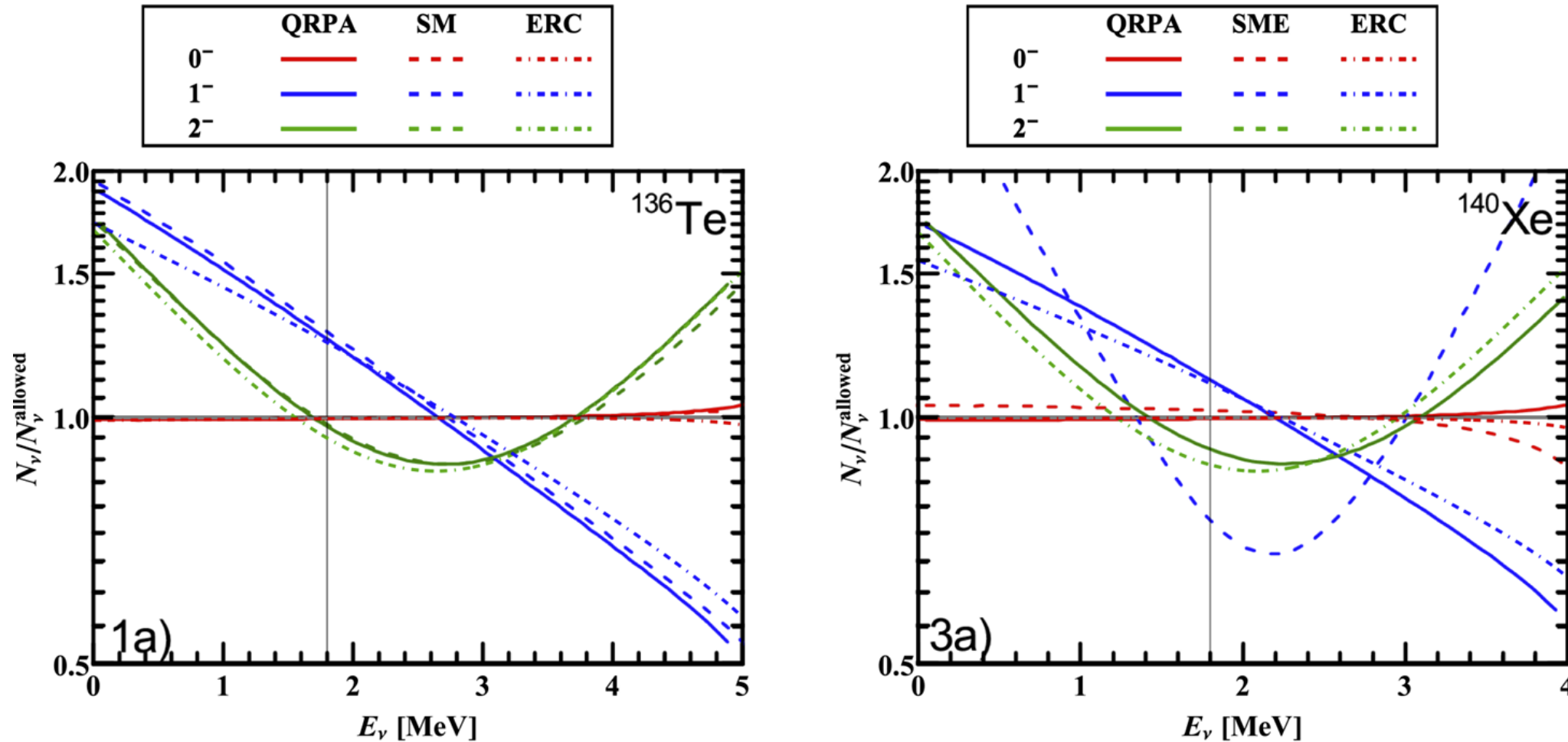
Forbidden shape factors



PRD 100 (2019) 5, 053005, YFL, Zhang

We choose **exact relativistic calculation (ERC)** from *Stefanik, Dvornicky and Simkovic (2017)*

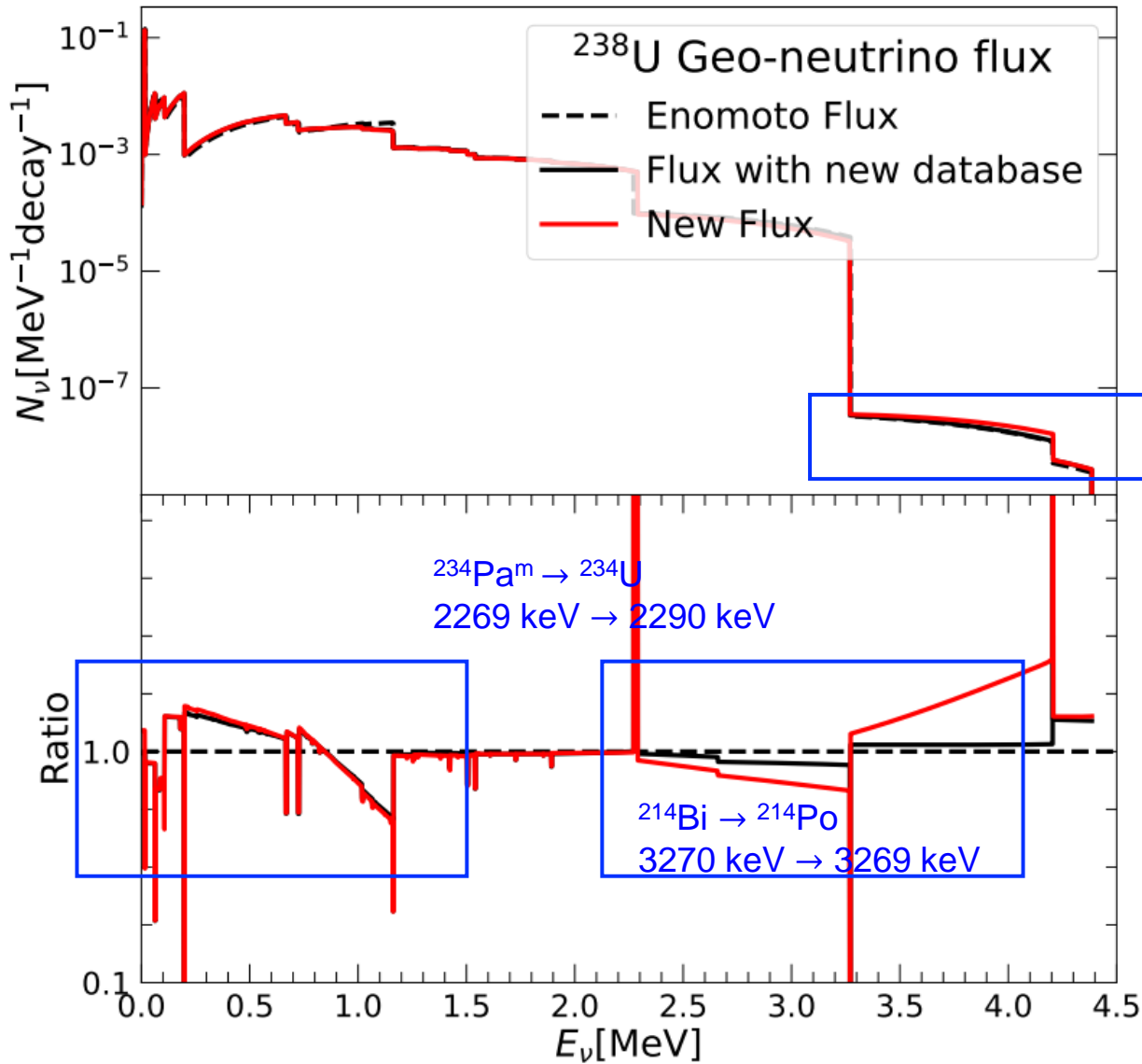
ERC v.s. Microscopic calculations



Here QRPA and SM microscopic calculations are from Fang & Brown (2015)

Phys.Rev.C 91 (2015) 2, 025503

Updated flux: update on database



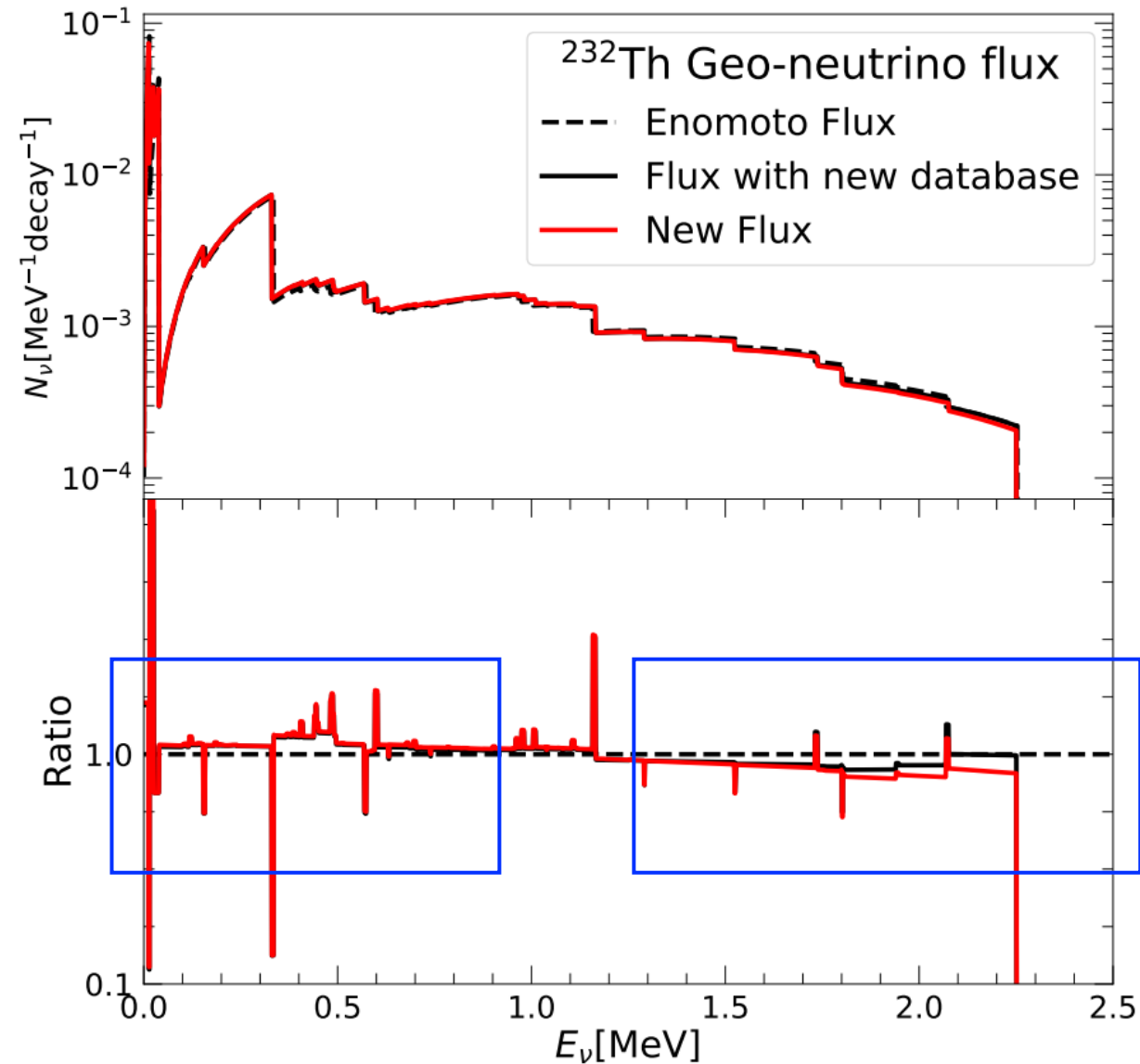
Flux with new database: calculated with ENSDF 2023

New flux: calculated with ENSDF 2023 + Forbidden decays + Higher-order corrections

$^{210}\text{Tl} \rightarrow ^{210}\text{Pb}$ not observed in neutrino experiments yet

- The extra beta branches in **low-energy region**
- Forbidden decays
 - $^{214}\text{Bi} \rightarrow ^{214}\text{Po}$ 1st non-unique forbidden ($\Delta J^\pi = 1^-$)
 - $^{234}\text{Pa}^m \rightarrow ^{234}\text{U}$ 1st non-unique forbidden ($\Delta J^\pi = 0^-$)

Updated flux: update on database



Flux with new database: calculated with ENSDF 2023

New flux: calculated with ENSDF 2023 + Forbidden decays + High-order corrections

- The extra beta branches in **low-energy region**
- Forbidden decays
 $^{212}\text{Bi} \rightarrow ^{212}\text{Po}$ 1st non-unique forbidden ($\Delta J^\pi = 1^-$)

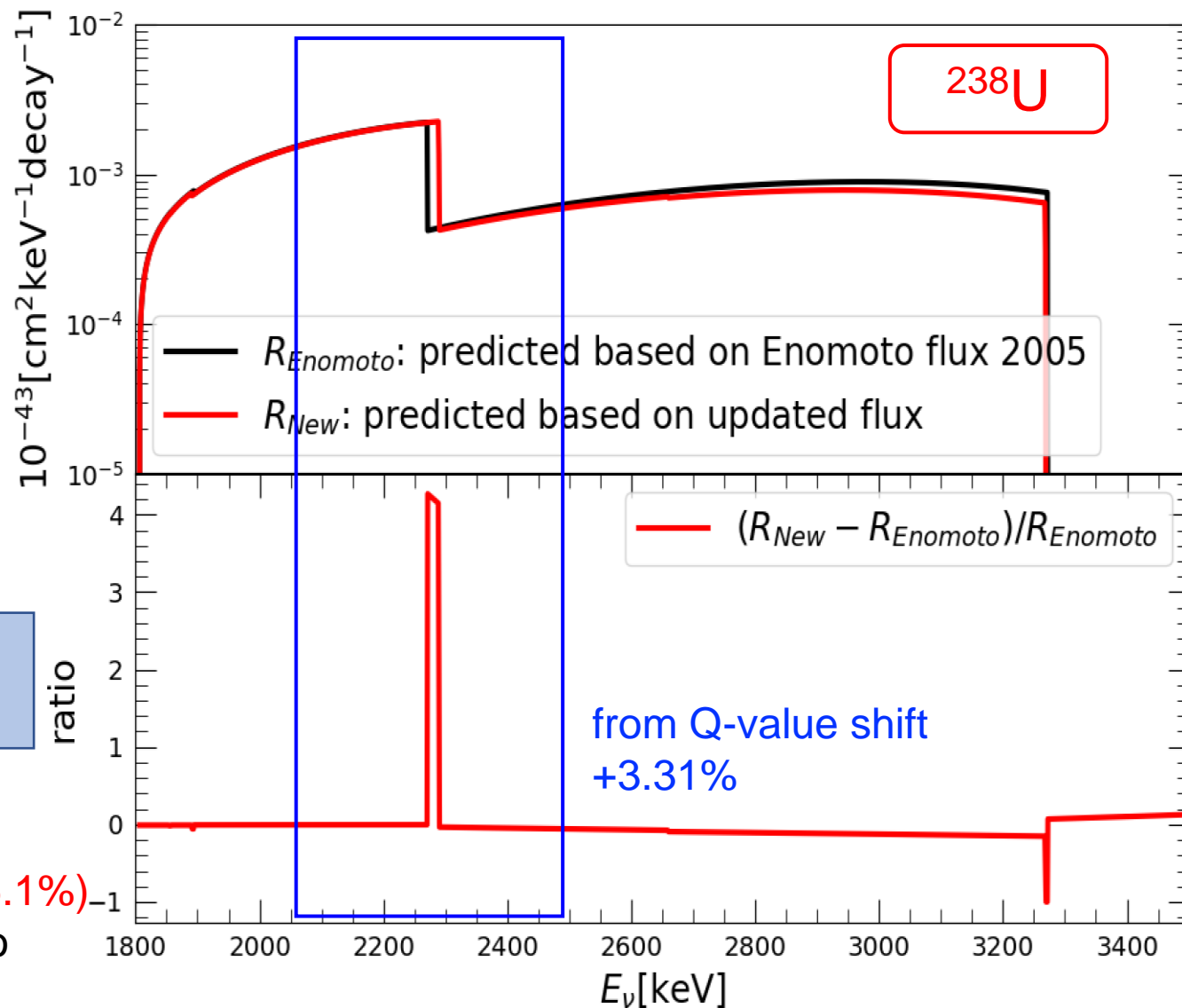
Prediction with IBD cross section



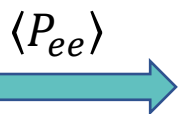
R_i means the **event rates** for different flux models (used $\langle P_{ee} \rangle$) is detected by σ_{SV}^{rc}

$$(R_{New} - R_{Enomoto})/R_{Enomoto}$$

	Database	forbidden decay+database
^{232}Th	-3.88 %	-9.00%
^{238}U	+0.16 %	-3.47%



Enomoto flux

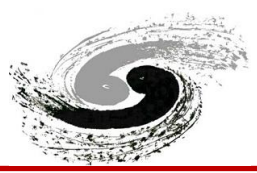


Strumia-Vissani +
radiative corrections

Updated flux

$$\sigma_{SV}^{rc}$$

The forbidden decays will bring additional $\sim -3.6\%$ (-5.1%) for ^{238}U (^{232}Th) geoneutrino estimation for geoneutrino event numbers.



The impact on the current and future exps.

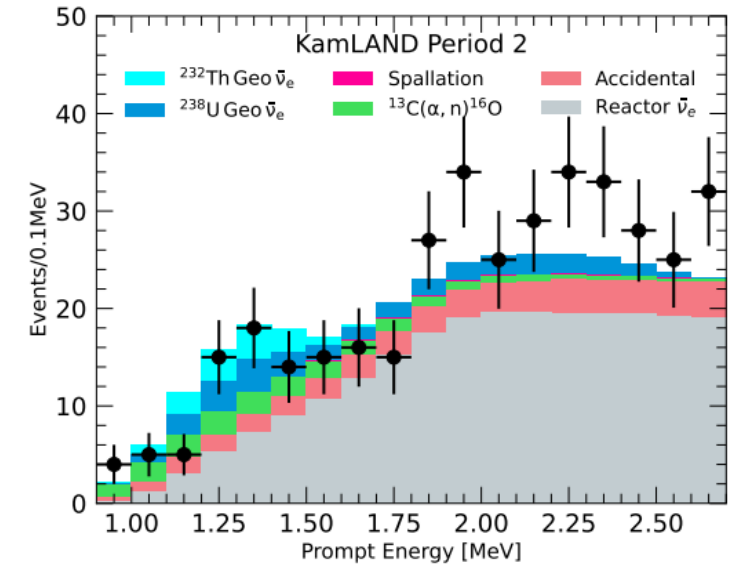
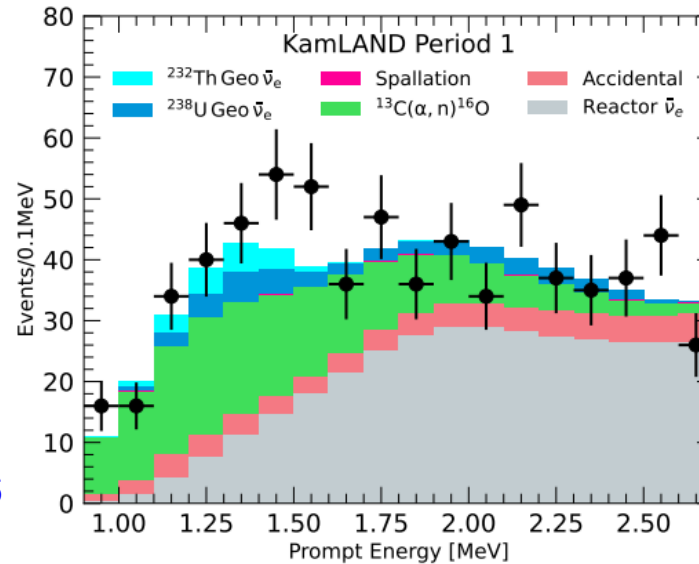
Observation in KamLAND & Borexino



KamLAND (2022)

- Liquid scintillator of 1 kon
- 18 years ~ 170 geo-neutrinos
- Precision
 - ~ 36% for ^{238}U
 - ~ 53% for ^{232}Th

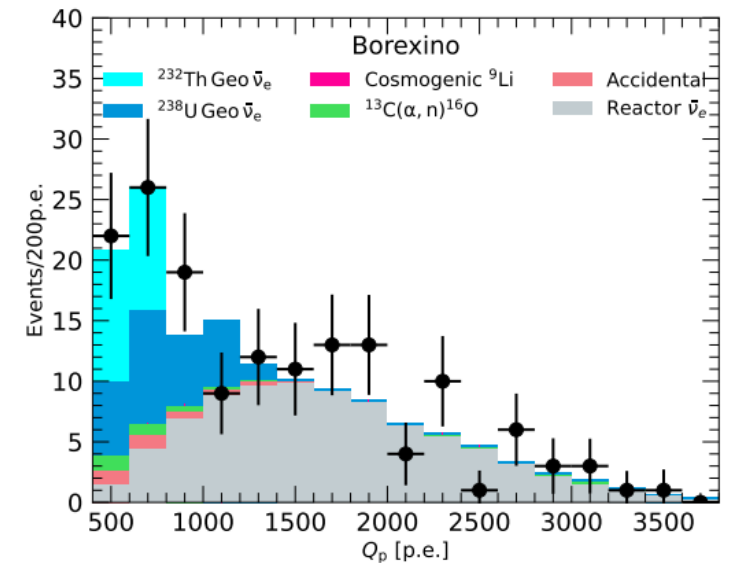
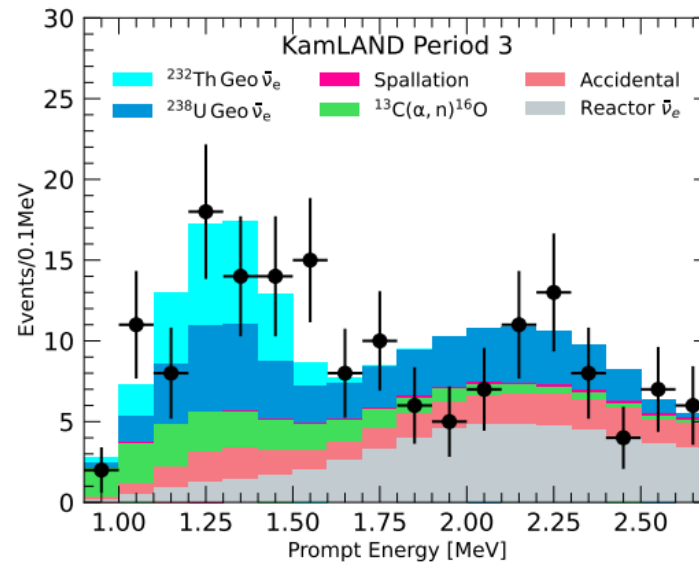
Geophysical Research Letters, 49, e2022GL099566



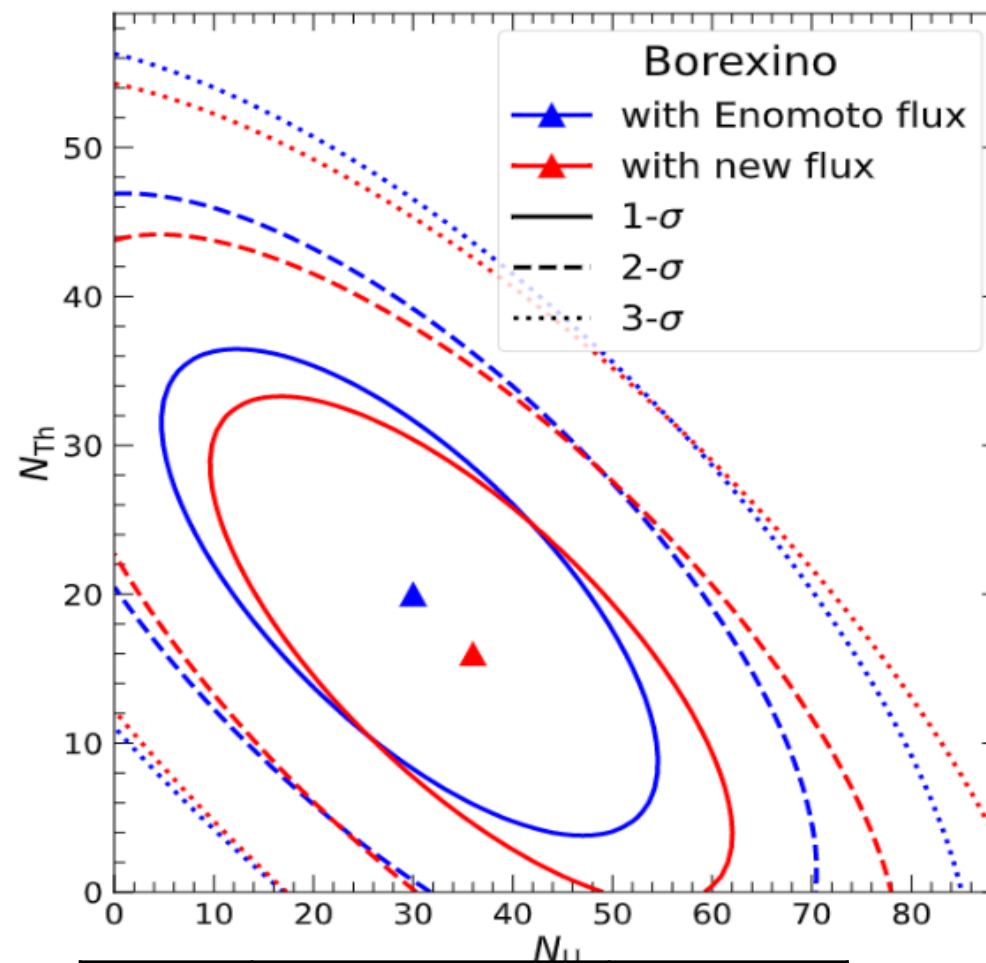
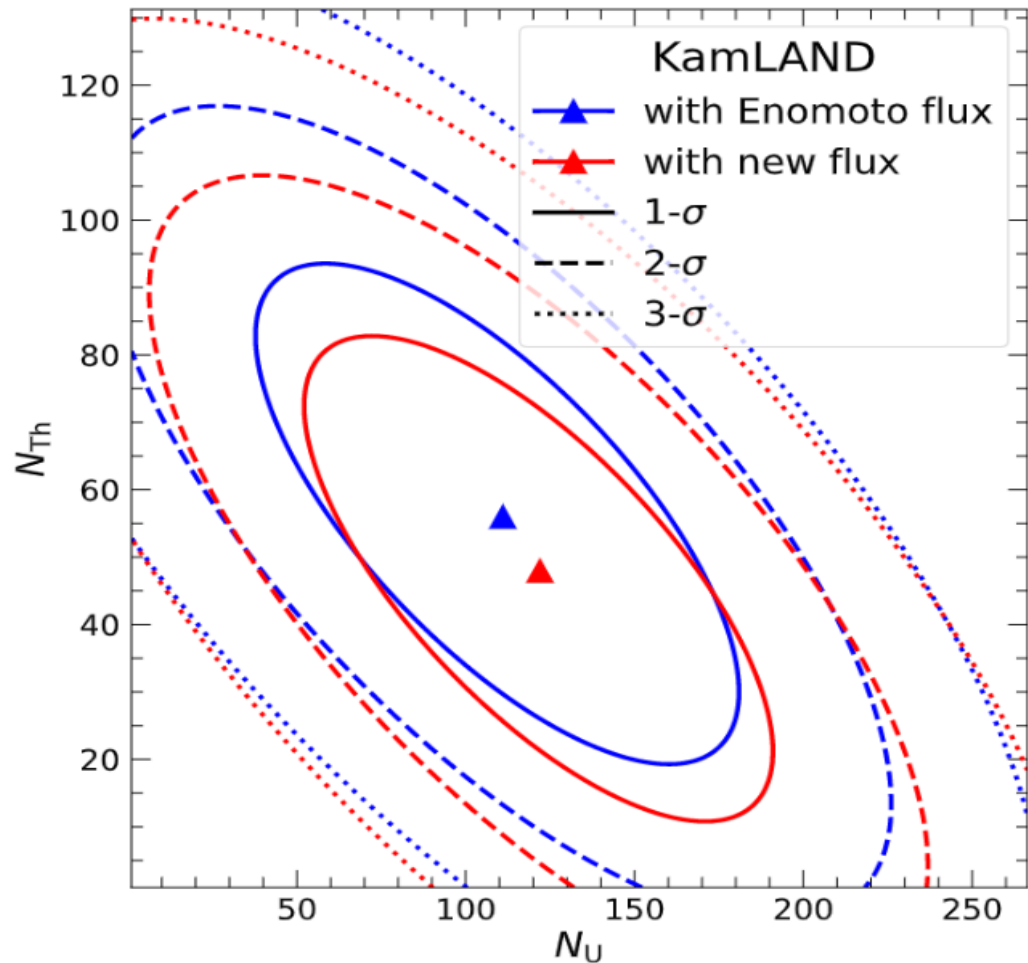
Borexino (2020)

- Liquid scintillator of 0.3 kon
- 10 years ~ 50 geo-neutrinos
- Precision
 - ~ 53% for ^{238}U
 - ~ 55% for ^{232}Th

Phys. Rev. D 101, 012009 (2020)



Impact on KamLAND and Borexino



	Enomoto's flux	New flux
N_{238}	111 ± 40 (36%)	122 ± 40
N_{232}	56 ± 30 (53%)	48 ± 28

+10% (0.3 σ deviation)

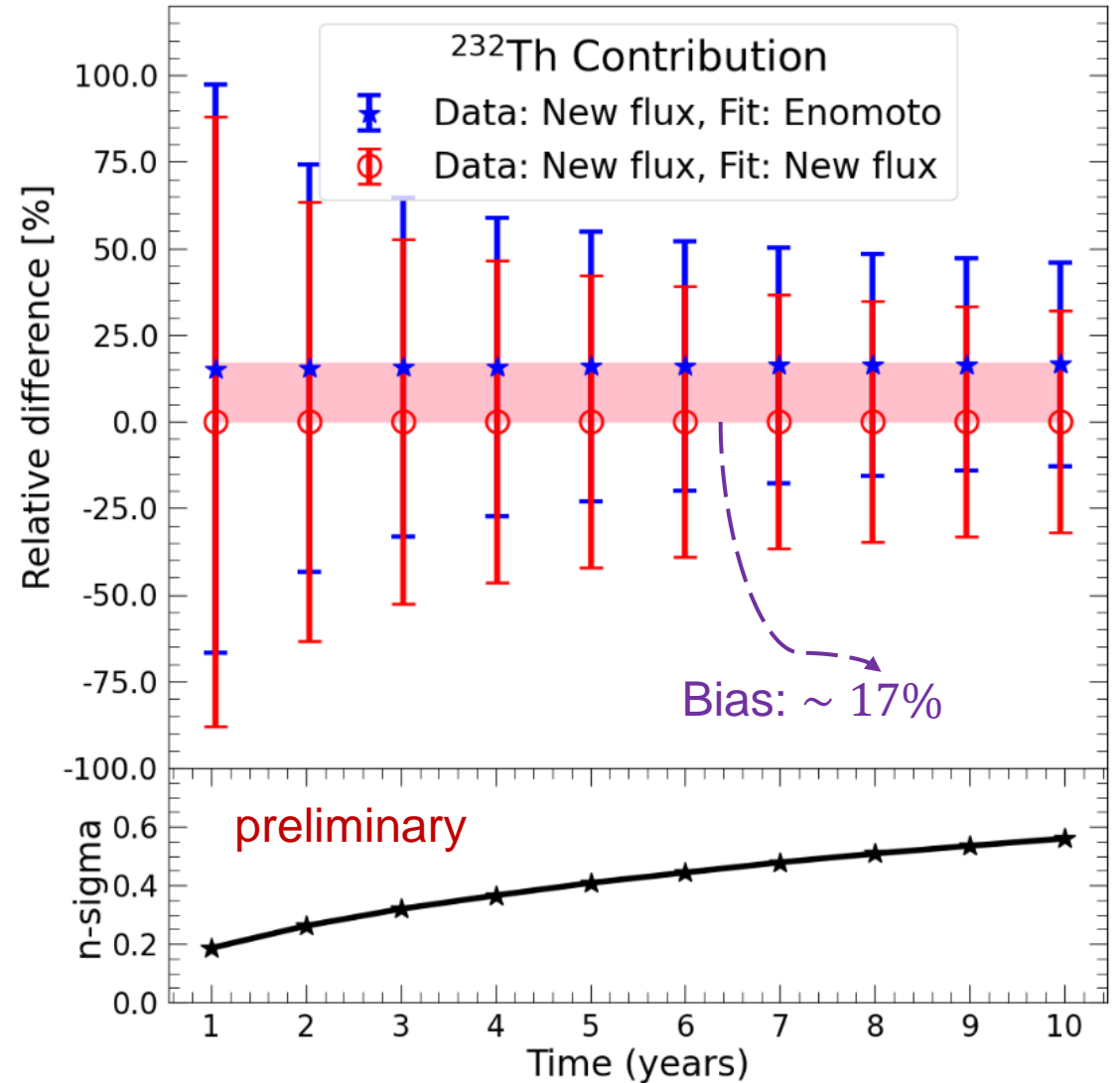
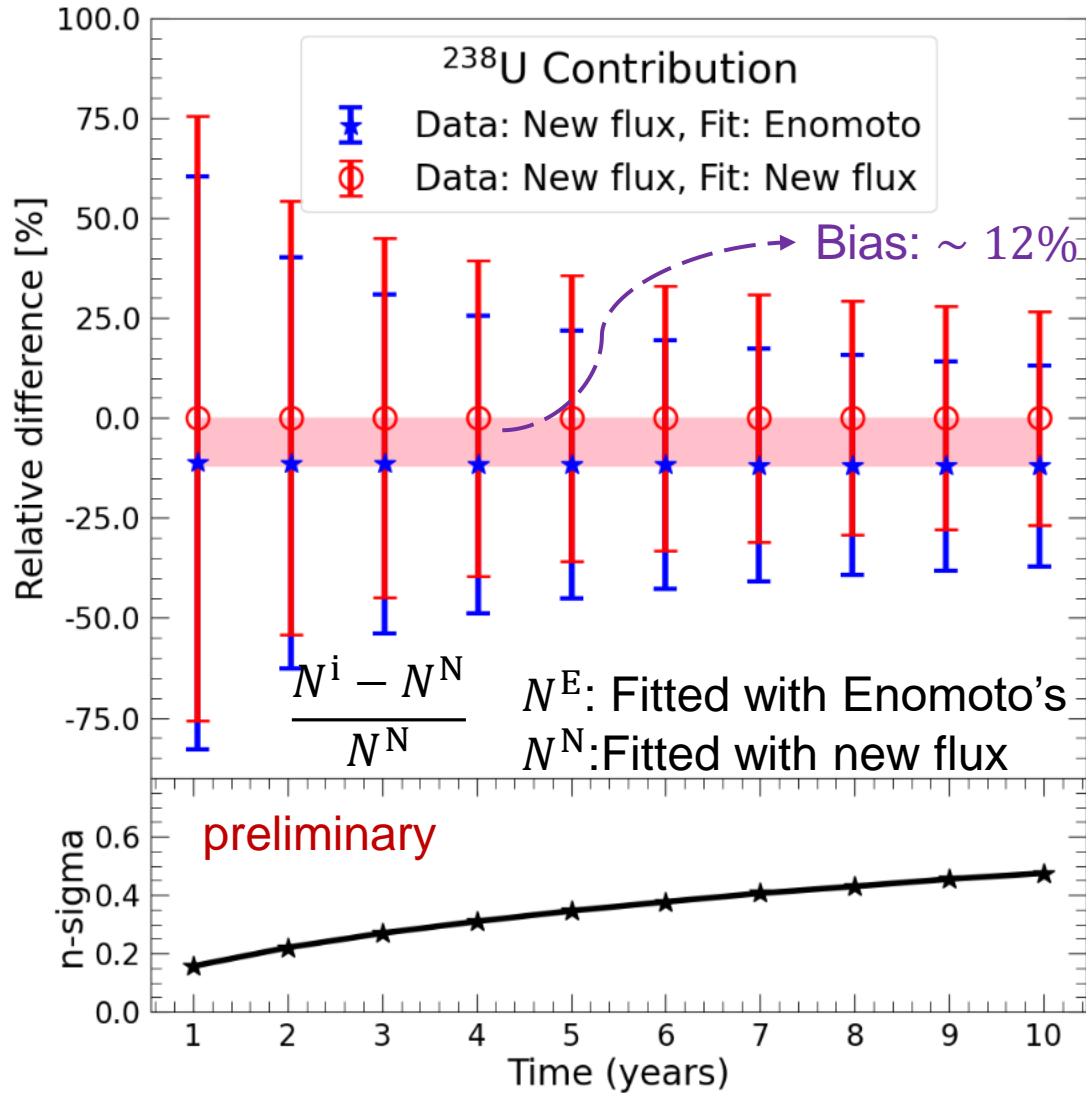
-16% (0.4 σ deviation)

	Enomoto's flux	New flux
N_{238}	30 ± 16 (53%)	36 ± 17
N_{232}	20 ± 11 (55%)	16 ± 11

+18% (0.4 σ)

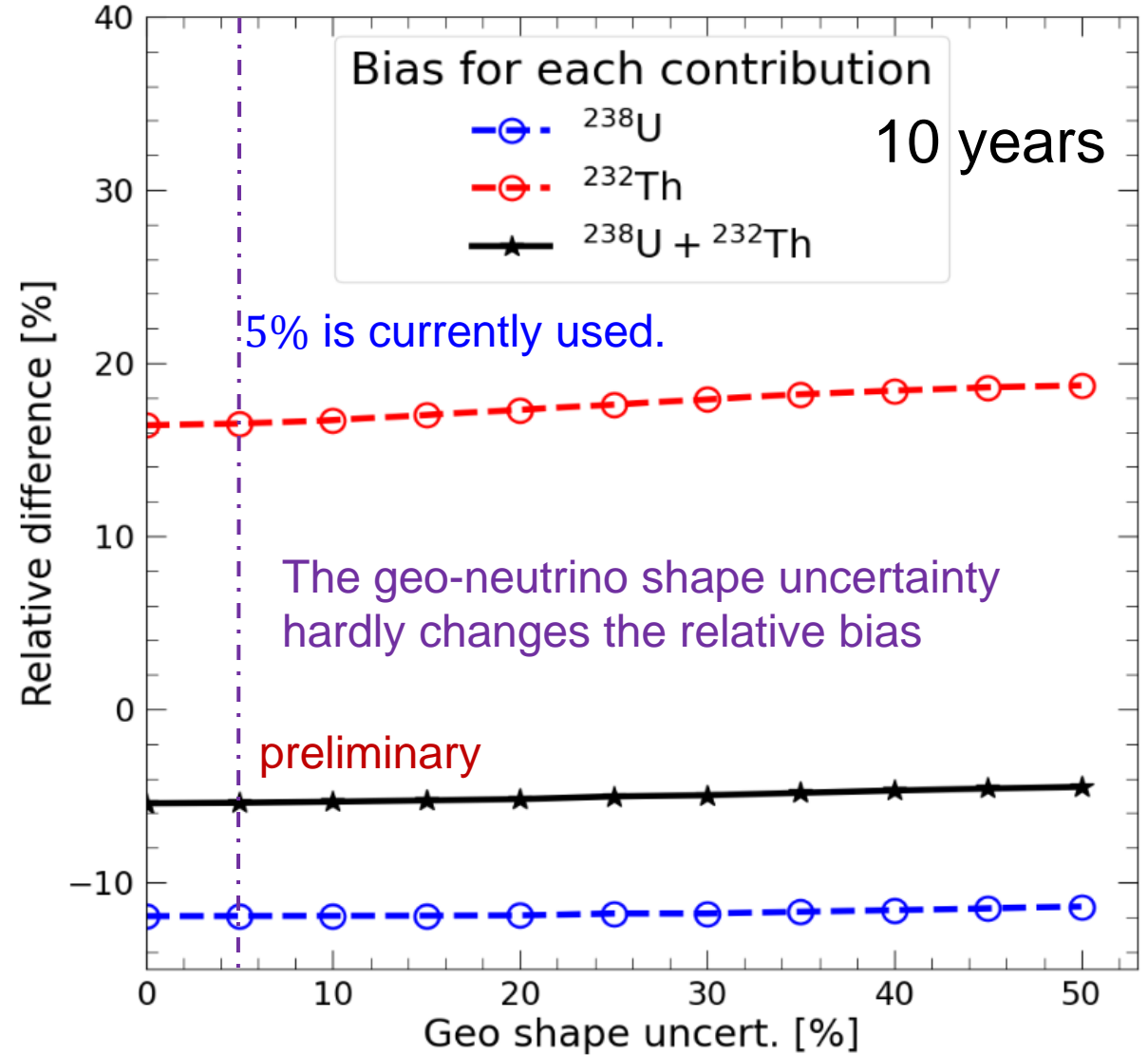
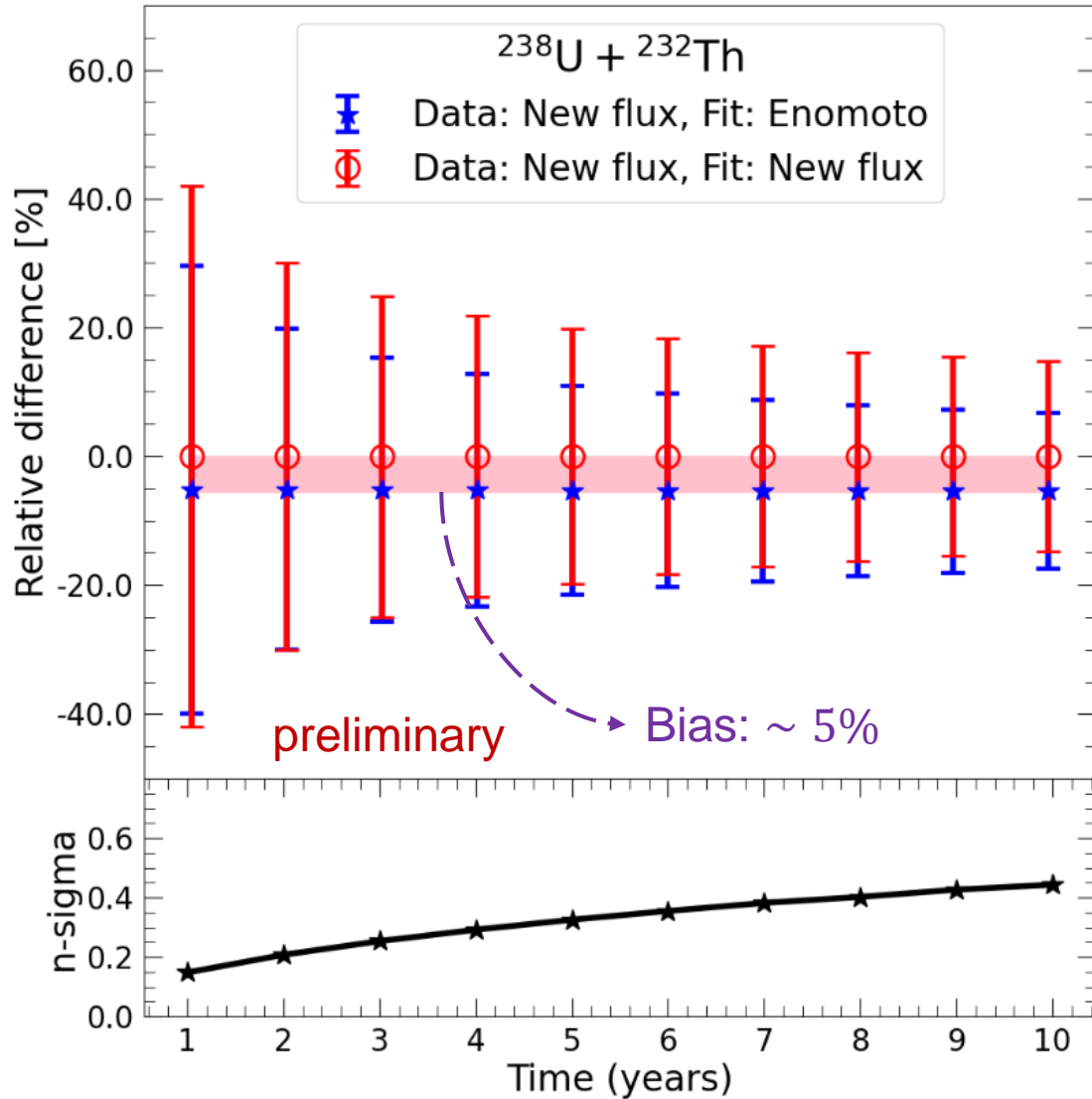
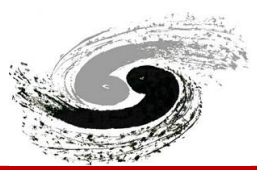
-22% (0.2 σ)

Sensitivity study (I)



The relative bias is unchanged as the significance (running time) will be increased.

Sensitivity study (II)



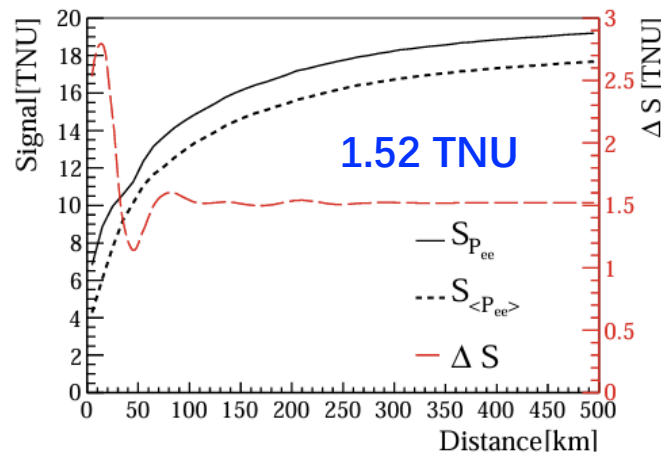
A related topic: oscillation effect



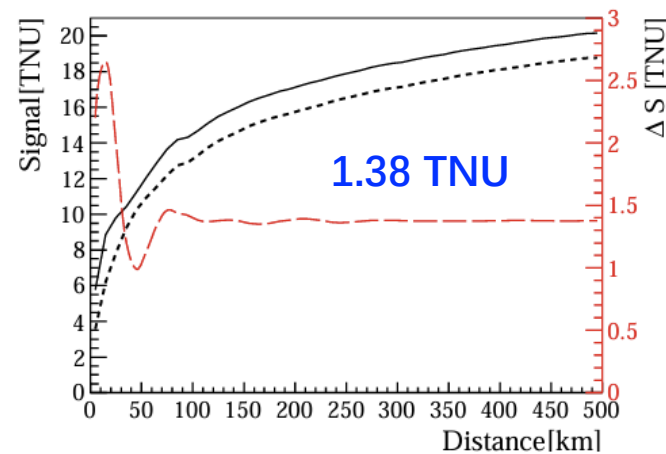
- Geo-neutrino is NOT a point source, but extended for the entire crust and mantle.
- Earlier studies neglected oscillation in the geo-neutrino prediction, but included a constant survival probability (approximation).

$$\langle P_{ee} \rangle \simeq \cos^4 \theta_{13} \left(1 - \frac{1}{2} \sin^2 2\theta_{12} \right) + \sin^4 \theta_{13} .$$

a) The rate would have a bias of around 1.5 TNU [Mao, Han, YFL, 1911.12302](#)



(a) KamLAND



(b) Borexino

b) The spectra exhibit variations of several percent when average probability is applied.

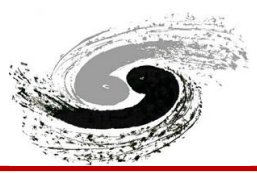
Conclusion



- A new geoneutrino flux model is presented.
 - based on new nuclear database: ENSDF 2023
 - including higher order corrections & forbidden decays
- IBD yields: ~10%, plus significant shape variation at high energy range
 - A Q value shift of 21 keV ($^{234}\text{Pa}^m \rightarrow ^{234}\text{U}$): 3.3%
- Forbidden shape factor is validated with microscopic calculations
 - Uncertainty evaluation
 - Direct measurements of Bi214/Bi212 at high energy range!
- Fitting with old flux may lead to bias to central value comparing with new flux model.
 - The relative bias almost keeps constant
 - ~ 10% – 20% for ^{238}U and ^{232}Th
 - ~ 5% – 10% for $^{238}\text{U}+^{232}\text{Th}$
 - Hardly changed by increasing geo shape uncertainty
 - The significance of the bias
 - ~ 0.5σ for current data
- Careful uncertainty quantification of the new geo flux model is on-going!



Thanks for your attention!



Backup

Observation in JUNO

Talk on Monday!



Geo-neutrino signals

- From the decay chains of ^{232}Th and ^{238}U
- About 1 event per day

Reactor neutrinos

- contributed by two near NPPs (52.5 km) and Daya Bay NPP (~200 km)

Neutrino selection efficiency: **82.2%**

	Rate [cpd]	Rate uncert.	Shape uncert.
Geo-neutrinos	1.2	-	5%
Reactor neutrinos	47.1	-	Daya Bay/ TAO
Accidental	0.8	1%	-
$^9\text{Li}/^8\text{He}$	0.8	20%	10%
$^{13}\text{C}(\alpha, n)^{16}\text{O}$	0.05	50%	50%
Fast neutron	0.1	100%	20%
World reactor neutrinos	1	2%	5%
Atmospheric neutrinos	0.16	50%	50%

World reactor neutrinos

- contributed by the NPPs (>300km)

JUNO will measure in 1y ~400 geo-neutrinos events more than Borexino and KamLAND in >10y!

Chin.Phys.C 46 (2022) 12, 123001

